

# Journal of Visualized Experiments

## Immunostaining of whole-mount retinas with the CLARITY tissue clearing method

--Manuscript Draft--

Article Type:	Methods Article - JoVE Produced Video
Manuscript Number:	JoVE62178R1
Full Title:	Immunostaining of whole-mount retinas with the CLARITY tissue clearing method
Corresponding Author:	Dao-Qi Zhang, Ph.D. Oakland University Rochester, Michigan UNITED STATES
Corresponding Author's Institution:	Oakland University
Corresponding Author E-Mail:	zhang@oakland.edu
Order of Authors:	Elizabeth Alessio Dao-Qi Zhang, Ph.D.
Additional Information:	
Question	Response
Please specify the section of the submitted manuscript.	Neuroscience
Please indicate whether this article will be Standard Access or Open Access.	Standard Access (US\$2,400)
Please indicate the <b>city, state/province, and country</b> where this article will be <b>filmed</b> . Please do not use abbreviations.	Rochester, Michigan, United States of America
Please confirm that you have read and agree to the terms and conditions of the author license agreement that applies below:	I agree to the <a href="#">Author License Agreement</a>
Please provide any comments to the journal here.	

## TITLE

Immunostaining of whole-mount retinas with the CLARITY tissue clearing method

## AUTHORS AND AFFILIATIONS

Elizabeth J. Alessio<sup>1</sup> and Dao-Qi Zhang<sup>1\*</sup>

<sup>1</sup>Eye Research Institute, Oakland University, Rochester, MI, USA

ejalessio@oakland.edu

\* Corresponding author:

Dao-Qi Zhang, Ph.D.

zhang@oakland.edu

## SUMMARY

Here we present a protocol to adapt the CLARITY method of the brain tissues for whole-mount retinas to improve the quality of standard immunohistochemical staining and high-resolution imaging of retinal neurons and their subcellular structures.

## ABSTRACT

The tissue hydrogel delipidation method (CLARITY), originally developed by the Deisseroth laboratory, has been modified and widely used for immunostaining and imaging of thick brain samples. However, this advanced technology has not yet been used for whole-mount retinas. Although the retina is partially transparent, its thickness of approximately 200  $\mu\text{m}$  (in mice) still limits the penetration of antibodies into the deep tissue as well as reducing light penetration for high-resolution imaging. Here, we adapted the CLARITY method for whole-mount mouse retinas by polymerizing them with an acrylamide monomer to form a nanoporous hydrogel and then clearing them in sodium dodecyl sulfate to minimize protein loss and avoid tissue damage. CLARITY-processed retinas were immunostained with antibodies for retinal neurons, glial cells, and synaptic proteins, mounted in a refractive index matching solution, and imaged. Our data demonstrate that CLARITY can improve the quality of standard immunohistochemical staining and imaging for retinal neurons and glial cells in whole-mount preparation. For instance, 3D resolution of fine axon-like and dendritic structures of dopaminergic amacrine cells were much improved by CLARITY. Compared to non-processed whole-mount retinas, CLARITY can reveal immunostaining for synaptic proteins such as postsynaptic density protein 95. Our results show that CLARITY renders the retina more optically transparent after the removal of lipids and preserves fine structures of retinal neurons and their proteins, which can be routinely used for obtaining high-resolution imaging of retinal neurons and their subcellular structures in whole-mount preparation.

## INTRODUCTION

The vertebrate retina is perhaps the most accessible part of the central nervous system (CNS), and it serves as an excellent model for studying the development, structure, and function of the brain. Five classes of neurons in the retina are distributed in three nuclear layers separated by two plexiform layers. The outer nuclear layer (ONL) consists of classical photoreceptors (rods and cones) that convert light into electrical signals. Electrical signals are processed by neurons in the inner nuclear layer (INL), including bipolar, horizontal, and amacrine cells, and then transmitted to retinal ganglion

cells (RGCs) in the ganglion cell layer (GCL). RGCs are the output neurons of the retina, with the axons projecting to the brain to contribute to image-forming and non-image-forming visual function. In addition, three types of glial cells (Muller cells, astroglia, and microglia) provide nutrients to neurons and protect neurons from harmful changes in their extracellular environment.

One specialized subpopulation of amacrine cells produces and releases dopamine, an important neuromodulator in the CNS, reconfiguring retinal neural circuits during light adaptation<sup>1,2</sup>. Dopaminergic amacrine cells (DACs) have a unique feature of morphological profiles. Their somata are located in the proximal INL with dendrites ramifying in the most distal part of the inner plexiform layer (IPL). Axon-like processes of DACs are unmyelinated, thin and long, sparsely branched, and bear varicosities (the sites of dopamine release). They form a dense plexus with dendrites in the IPL, including ring-like structures around the somata of All amacrine cells. The axons also run through the INL toward the OPL, forming a centrifugal pathway across the retina<sup>3</sup>. We have demonstrated that DAC processes express receptors in response to glutamate release from presynaptic neurons, including bipolar cells and intrinsically photosensitive retinal ganglion cells (ipRGCs)<sup>4-6</sup>. However, it is unclear whether glutamate receptors express on the axons, dendrites, or both since they are cut off in vertical retinal sections and cannot be distinguished from each other<sup>5,6</sup>. Immunostaining needs to be carried out in whole-mount retinas to reveal three-dimensional branching of DACs and the presence of glutamate receptors on subcellular compartments. Although the retina is relatively transparent, the thickness of a mouse whole-mount retina is approximately 200  $\mu\text{m}$ , which limits the penetration of antibodies into the deep tissue as well as reduces light penetration for high-resolution imaging due to tissue light-scattering. To overcome these limitations, we adapted the immunostaining compatible tissue hydrogel delipidation method (CLARITY) developed recently for thick brain sections to whole-mount mouse retinas<sup>7</sup>.

The CLARITY method was originally developed by the Deisseroth laboratory for immunostaining and imaging of thick brain samples<sup>7</sup>. It uses a strong detergent, sodium dodecyl sulfate (SDS) and electrophoresis to remove the lipid components (that cause tissue light-scattering), leaving the proteins and nucleic acids in place. The removed lipids are replaced with a transparent scaffold made up of hydrogel monomers such as acrylamide to support the remaining protein structure. The cleared tissue can be labeled via immunohistochemistry and imaged with substantially increased light penetration depth through the tissue (up to several millimeters below the tissue surface). Since then, the CLARITY method has been optimized and simplified by several research groups<sup>8-10</sup>. A modified CLARITY protocol uses a passive clearing technique to avoid the possible tissue damage produced by electrophoresis for clearing the whole-brain and other intact organs<sup>11</sup>. However, this method has not yet been applied to whole-mount retinas. Here, we adapted the passive CLARITY technique for whole-mount retinas to make them more transparent for immunohistochemistry and imaging. We found that a majority of the retinal proteins tested were preserved during this process for immunohistochemistry. Using the refractive index matching solution, we were able to image retinal neurons across the approximately 200  $\mu\text{m}$  thickness from the ONL to the GCL in whole-mount retinas.

## PROTOCOL

Mouse care and all experimental procedures were conducted according to the National Institutes of Health guidelines for laboratory animals and were approved by the Institutional Animal Care and Use Committees at Oakland University (protocol no. 18071).

NOTE: Names of the solutions and their compositions are listed in **Table 1**.

## **1. Tissue preparation**

1.1 Euthanize the mouse with an overdose of CO<sub>2</sub>, followed by cervical dislocation.

1.2 Enucleate the eyes with curved forceps and transfer them to a small petri dish with 0.1 M PBS (**Table 1**). Under a dissection microscope, poke a small hole along the cornea-sclera junction with a needle. Transfer to 4% paraformaldehyde (PFA) for 1 hour.

1.3 Transfer the eye back to a dish with PBS. Under a dissection microscope, use dissection scissors to cut all the way around the cornea-sclera junction. Remove the cornea and lens. Cut at the base of the optic nerve and carefully peel the sclera off with forceps to isolate the retina.

1.4 Make four small cuts evenly around the retina and use a fine tip brush dipped in PBS to lay it flat (GCL side down) in a clover-like shape on a small square cut from nitrocellulose filter paper to stabilize the retina.

1.5 Transfer the retina using forceps to hold the corner of the nitrocellulose paper (without touching the mounted retina) and place it in a 48-well plate with 4% PFA for 1 hour.

1.6 Transfer the filter paper and retina to a well with PBS and wash (3x for 5 min each).

1.7 Transfer to A4P0 (**Table 1**) and incubate overnight at 4 °C with gentle agitation.

1.8 Pipette vegetable oil into the well to completely cover the A4P0 solution. Incubate in a water bath at 40 °C for 3 hours with no shaking.

1.9 Wash (3x for 5 min each) in PBS, making sure all the oil has been rinsed off. If necessary, use a pipet to carefully remove remaining oil from the top of the well before the last rinse.

1.10 Incubate in 10% SDS at 40 °C for two days with gentle shaking. Replace SDS with fresh solution on the second day.

1.11 Transfer the filter paper and retina to PBS with Triton-X-100 (PBST, **Table 1**) and wash (5x for 1.5 h each).

1.12 Store at 4 °C in PBST with 0.01% sodium azide (NaN<sub>3</sub>) or move directly to immunostaining.

## **2. Immunostaining and refractive index matching**

2.1 Remove the retina from the filter paper by gently peeling it off with a fine tip brush in PBST.

2.2 Incubate the retina in primary antibody (**Table 2**) diluted in blocking solution (**Table 1**) for 2 days at 40 °C with gentle shaking.

2.3 Wash (5x, 1.5 h each) in PBST.

2.4 Incubate with the appropriate secondary antibodies (**Table 3**) diluted in blocking solution for 2 days at 40 °C with gentle shaking and protect from light through the remainder of the procedure.

2.5 Wash (5x, 1.5 h each) in 0.02 M phosphate buffer (see **Table 1**).

2.6 Incubate in sorbitol-based Refractive Index Matching Solution (sRIMS, see **Table 1**) at 40 °C overnight with gentle shaking.

### 3. Mounting

3.1 Outline a 18 mm x 18 mm x 1.5 mm glass coverslip with a fine-tip permanent marker to mark a square boundary on the back of a glass microscope slide.

3.2 Flip the slide over and use a syringe to trace the boundary with a thin line of silicone grease on the front of the slide, leaving a small gap in one corner for excess mounting solution to escape.

3.3 Transfer the retina to the center of the bounded area and arrange with a fine-tip brush so that it lies flat with the photoreceptor side against the glass slide.

3.4 Pipette approximately 60 µL of sRIMS so that it covers the flattened retina and extends to one corner of the enclosure, taking care that the retina stays flat and in place.

3.5 Apply the coverslip starting from the corner with the sRIMS and slowly lower it until it touches the grease on all sides, avoiding the formation of air bubbles.

3.6 Place a stack of 3 coverslips on each side of the mounted retina as a spacer. Use the long edge of another slide to press down the coverslip so that the mount is flat and even.

3.7 Store slides flat at 4 °C until imaging.

### 4. Imaging

4.1 Image samples on either a conventional fluorescence microscope or a confocal microscope (**Table of Materials**). Begin by placing the slide on the microscope stage and locating the sample.

NOTE: If an inverted objective microscope is being used, place the slide upside down on the stage, first ensuring that the exposed areas of the slide are clear of all silicone grease and mounting solution.

4.2 To obtain z-stacked images of co-labeled samples, first focus on the signal in each channel individually and set the exposure time or scanning speed, for fluorescence or confocal microscopes, respectively.

4.3 Set the range for the z-stack either by manually setting the focal plane at the top and bottom of the desired range, or by setting the midpoint and then specifying a range around the midpoint.

4.4 Adjust the step size or number of slices as desired.

4.5 Capture the image and save the original file as well as exporting it as a TIFF file or other desired format.

## 5. Image analysis

5.1 Use the image analysis software of choice (**Table of Materials**) to adjust the brightness and contrast in each channel until optimum clarity is achieved in both the single images and the 3-dimensional rendering of the z-stack.

NOTE: If the selected step size is sufficiently small, 3D deconvolution can also be performed to enhance the signal.

## REPRESENTATIVE RESULTS

### Modified CLARITY-processed retinas are optically transparent tissue.

To formulate a tissue clearing method that is compatible with immunohistochemical applications in the retina while providing adequate delipidation and retaining the structural integrity of the cellular proteins, we adapted the CLARITY tissue clearing method to whole-mount mouse retinas. We were able to simplify the protocol and modify it for whole-mount retinas (see Protocol). After completing tissue hybridization, clearing, and refractive index matching, retinas processed with this modified CLARITY protocol showed almost complete optical transparency throughout the thickness of the retina (**Figure 1A**) when compared to non-processed control retinas (**Figure 1B**). This result indicates that this modification of the CLARITY protocol provides sufficiently cleared whole-mount retina tissue.

### Improved 3D imaging of neurons in modified CLARITY processed retinas

To assess the quality and practicality of immunohistochemical staining afforded by this modified CLARITY method, we stained CLARITY processed retinas with various primary antibodies (**Table 2**). These antibodies mark each major cell type in the retina: cone photoreceptors, rod bipolar cells, amacrine cells, RGCs, and glial cells, as well as antibodies against subcellular synaptic proteins. With the exception of the cell activity marker phospho-S6 (pS6), all antibodies tested proved to be compatible with CLARITY. Typical examples are illustrated in **Figure 2**. We performed triple labeling with antibodies against cone arrestin, tyrosine hydroxylase (TH), and RNA-Binding Protein with Multiple Splicing (RBPMs). We took a series of z-stack confocal microscopy images from the ONL to the GCL. Individual images showed the arrestin labeled cones in the ONL (**Figure 2A**), TH-labeled DACs in the INL (**Figure 2B**) and RBPMs-marked RGCs in the GCL (**Figure 2C**). An overlay image revealed the relative location of these neurons throughout the entire thickness of the retina (**Figure 2D**). These results suggest that CLARITY can improve the quality of many standard

immunohistochemical staining and clearly reveal the 3D structure of neurons across the entire thickness of the retina in whole-mount preparations.

### **Modified CLARITY provides improved 3D resolution of fine processes of retinal neurons and synaptic proteins.**

We further analyzed TH staining in CLARITY-processed whole-mount retinas (**Figures 3A,B**) and compared it to imaging obtained from standard whole-mount preparation (**Figures 3C,D**). Confocal images show that dendrites and axon-like processes of DACs were revealed much more clearly in a CLARITY processed retina (**Figure 3A**) than in a standard retina (**Figure 3C**). In particular, axon-like processes of DACs exhibited more complete ring-like structures in a CLARITY retina (see an insert in **Figure 3A**) than in a standard retina (see an insert in **Figure 3C**). Notably, ring-like structures of a CLARITY retina taken using fluorescence microscopy (**Figure 3B**) were almost identical to those observed using confocal (**Figure 3A**). In addition, axon-like processes also ran toward the outer retina, which was observed in X-Z oriented images (**Figure 4A**). These data suggest that CLARITY can be used to identify axon-like processes of DACs in whole-mount retinas even with the use of conventional fluorescence microscopy.

When the AMPA-receptor subunit GluA2 and postsynaptic density protein 95 (PSD-95) were examined in standard whole-mount retinas, neither of them were detected, likely due to poor penetration of antibodies against these synaptic proteins into the deep retina. To determine whether CLARITY-processed retinas allow these antibodies to immunostain synaptic proteins, we triple labeled TH with the subunit GluA2 and PSD-95. Immunostaining against GluA2 and PSD-95 showed distinct puncta revealing individual GluA2-containing AMPA receptors (**Figure 4B**) and putative postsynaptic sites (**Figure 4C**), respectively. An overlay image showed some puncta apparent on DAC processes (**Figure 4D**). We imaged a point of putative colocalization with all three stains and presented it in 3D views (**Figure 5**). From all three views, TH colocalized clearly with both GluA2 and PSD-95 (**Figure 5 A-C**). These 3D perspective results from whole-mount retinas validate our previous reports of synaptic expression of GluA2-containing AMPA receptors on DAC processes in vertical retinal slices.

### **FIGURE LEGENDS**

**Figure 1. CLARITY provides optically transparent tissue.** Whole-mount mouse retinas were processed with the modified CLARITY method (see Protocol) and the entire retina imaged with a dissection microscope, overlaid on a 0.67 cm square grid to show scale. **A:** CLARITY-processed whole-mount retina, with grid lines clearly visible through the transparent tissue. Arrows delineate the placement of the retina. **B:** Non-CLARITY-processed control retina, fixed in PFA for 1 h and incubated in PBS. Grid lines are obscured by the relative opacity of the tissue. Scale bar: approximately 2 mm.

**Figure 2. Improved 3D imaging of neurons across the thickness of the retina in CLARITY-processed retinas.** Whole-mount CLARITY retinas were immunostained with antibodies against cone arrestin, TH, and RBPMS. Image represents a 3D volume rendering of a z-stacked confocal image, viewed in an X-Z orientation. **A:** Cone photoreceptors (arrow) labeled by cone arrestin (blue). A slight speckle is visible in the inner retina (arrowheads), likely due to background staining. **B:** DAC soma and dendrites (arrow) labeled by TH (red). Arrowheads indicate retinal blood vessels in the inner retina, visible due to the multi-label immunostaining. **C:** RGC somata (arrow) labeled by RBPMS (green). Arrowheads indicate retinal blood vessels visible due to autofluorescence and non-specific staining

of blood vessels. **D:** Merged image of the triple labeled staining, revealing the relative placement of these neurons across the thickness of the retina, with cone photoreceptors located in the outer nuclear layer, DACs in the inner nuclear layer, and RGCs in the ganglion cell layer. Scale of the volume view is marked in increments of 20  $\mu\text{m}$ .

**Figure 3. CLARITY reveals fine structures of DAC morphology.** TH immunostaining was performed in CLARITY-processed (**A** and **B**) and standard (**C** and **D**) retinas. Z-stacked images were taken using confocal (**A** and **C**) and fluorescence microscopy (**B** and **D**). An insert from a single optical plane in each image highlights ring-like structures presumably formed by axon-like processes. Arrowheads indicate DAC somata, and many ring-like structures are visible (examples are indicated by arrows) in the dense plexus of dendrites and axon-like processes revealed in CLARITY-processed retinas (**A** and **B**).

**Figure 4. Modified CLARITY provides improved 3D resolution of fine dendritic structures and synaptic proteins.** Triple immunostaining was performed in CLARITY-processed whole-mount retinas with antibodies against TH, GluA2, and PSD-95. A volume rendering was reconstructed from z-stacked confocal imaging and presented in an angled X-Z orientation. **A:** TH-labeled DAC somata (arrowheads) in the inner nuclear layer and processes (yellow arrows) stratifying in the distal inner plexiform layer (red). White arrows indicate centrifugal processes extending toward the outer retina. **B:** Dense punctate expression of GluA2-containing AMPA receptors across the inner plexiform layer (green). Arrow indicates autofluorescence from a retinal blood vessel. **C:** Puncta revealing post-synaptic sites labeled by PSD-95 in the inner plexiform layer (blue). Arrows indicate blood vessels, apparent due to the use of a mouse monoclonal antibody against PSD-95. **D:** Overlay image demonstrating overlap of the TH-labeled DAC processes with the expression of GluA2 and PSD-95. Scale of the volume view is marked in increments of 20  $\mu\text{m}$ .

**Figure 5. Synaptic expression of GluA2-containing AMPA receptors on DACs.** A point of putative triple colocalization of TH, GluA2, and PSD-95 shown in Figure 4 was selected and investigated in 3D. A1 represents a segment of a DAC process (red) in the X-Z orientation (A5). A2 and A3 show a single GluA2 punctum (green) and PSD-95 punctum (blue), respectively, in the same orientation. The merged image (A4) demonstrates triple colocalization of TH, GluA2 and PSD-95 (arrow). B1-B4 show the same point of colocalization (arrow) in a Y-Z orientation (B5). C1-C4 show colocalization of the same point (arrow) in the X-Y plane (C5). Triple colocalization is clearly apparent in each orientation. Scale bar: 2  $\mu\text{m}$ .

## TABLE LEGENDS

**Table 1. Composition of solutions.**

**Table 2. Summary of primary antibodies tested.** IHC legend: +3 = consistent, highly specific staining; +2 = consistently good staining, minimal background; +1 = good staining, some background; 0 = incompatible with CLARITY.

**Table 3. Summary of secondary antibodies tested.**

## DISCUSSION

**Modification of the CLARITY protocol for whole-mount retinas.**



We have simplified the CLARITY protocol to achieve adequate polymerization without the need for a vacuum evacuation or desiccation chamber, as is used in most previous studies<sup>7,9,11</sup>. The polymerization process is inhibited by oxygen, requiring that the sample be isolated from air during the polymerization step of the protocol. However, rather than degassing with nitrogen, we found that covering the sample with oil sufficiently isolated the sample to allow polymerization without adversely affecting the remainder of the protocol after a thorough rinse, as previously documented<sup>12</sup>. We further simplified the protocol with a passive clearing method to limit the risk of tissue browning and damage to tissue structure associated with electrophoretic clearing<sup>11</sup>. The passive clearing is accelerated by gentle agitation and elevated temperature, allowing complete tissue clearing in only two days. During this time period, sufficient delipidation is achieved to result in optically transparent tissue while minimizing the loss of proteins and other biomolecules integral to cellular structure and immunohistochemical staining.

### **CLARITY preserves proteins of retinal neurons and glial cells in whole-mount preparations.**

Our results show that almost all antibodies tested work in CLARITY processed retinas. These antibodies mark photoreceptors, bipolar cells, amacrine cells, RGCs and glial cells. Although we were not able to test antibodies for subtypes of each class of retinal neurons, our results imply that CLARITY processed retinas can be used for the majority of cellular markers in the retina. Although most antibodies we tested can also immunostain retinal neurons in non-CLARITY processed retinas, we found that CLARITY allowed adequate antibody penetration into the deep tissue of the retina, providing good specificity of staining in the middle layer of the retina. Additionally, we found that CLARITY improved light penetration throughout the thickness of the retina, reducing light scattering and allowing high-resolution imaging through even the deepest layers. These factors contribute to an improvement in both staining and imaging in the CLARITY-processed whole-mount retinas compared to non-CLARITY standard whole-mount IHC<sup>13</sup>. The reduced background and improved 3D imaging and volume renderings allow a complete investigation of cellular structures throughout all layers across the thickness of the retina.

### **CLARITY reveals fine processes and synaptic structure of DACs in whole-mount retinas.**

Our results demonstrate that ring-like structures and centrifugal processes of DACs are revealed in CLARITY-processed better than in non-CLARITY whole-mount retinas. In particular, immunostaining with CLARITY-processed tissue allows for good resolution of these fine structures even with standard fluorescence microscopy without the need for confocal imaging. Given the importance of DACs in visual function, the CLARITY preparation can be used to investigate DACs' structures in normal retinas and morphological changes under diseased conditions.

Upon immunostaining for PSD-95 and GluR2 with standard wholemount tissue, we observed little to no labeling of these subcellular structures in the deep layers of the retina, indicating poor antibody penetration. The application of the CLARITY protocol allows distinct staining of these proteins in the inner retinal layers, indicating improved antibody penetration to the deep tissue. Our results show that CLARITY allows the detection of synaptic proteins on DAC processes in whole-mount retinas, which is normally observed in vertical slice preparations<sup>6</sup>. Since axon-like processes cannot be distinguished from dendrites in vertical slices, CLARITY whole-mount retinas provide an opportunity to determine whether synaptic inputs to DACs from other neurons such as bipolar cells and ipRGCs occur in dendrites, axon-like processes, or both<sup>5,6</sup>. Since AMPA receptors and PSD-95 proteins are

widely distributed throughout the IPL, the expression of these proteins on DACs set an excellent example for CLARITY retinas to be used for identification of synaptic proteins in other retinal neurons.

### **Considerations, limitations, and future applications of the CLARITY protocol for whole-mount retinas.**

First, the polymerization and clearing protocols for CLARITY-processed whole-mount retinas add several days to the tissue preparation process. However, the method is still made highly practical by the fact that clarified retinas can be stored in sodium azide-containing PBS for up to two weeks with minimal tissue degradation. Second, some expansion of the tissue was observed throughout the clearing process as documented in previous applications of CLARITY<sup>7,11</sup>. However, we found that the retina returned to approximately original size upon equilibration with the refractive index matching solution. The potential minor changes in tissue volume may not cause significant distortion of cellular or subcellular structure<sup>7,11</sup>. Third, when imaging thicker brain samples, the microscope objective is often immersed directly in the mounting media to allow complete refractive index matching from the microscope lens through the tissue<sup>12</sup>. With thinner samples such as the retina, we used coverslips for mounting to make the samples flatter and more even for imaging. The effects of refraction through the coverslip appear to be minimal on imaging. Fourth, some of our images show non-specific blood vessel staining because we did not perfuse the whole animal with intracardiac perfusion (suggested to be used to avoid non-specific staining) before enucleating the eyes. Lastly, the current protocol adapted for mice can be used for retinas of other species. In particular, retinas of large animals such as dogs, pigs, horses and primates are much thicker than those of mice. This CLARITY protocol could render retinas of these animals more optically transparent after the removal of lipids and preserve the fine structures of retinal neurons and their proteins for immunostaining.

### **ACKNOWLEDGEMENTS**

We would like to thank Bing Ye, Nathan Spix, and Hao Liu for technical support. This work was supported by the National Institute of Health Grants EY022640 (D.-Q.Z.) and Oakland University Provost Undergraduate Student Research Award (E.J.A.).

### **DECLARATION OF INTERESTS**

The authors declare no competing financial interests.

### **REFERENCES**

- 1 Witkovsky, P. Dopamine and retinal function. *Documenta Ophthalmologica*. **108** (1), 17-40 (2004).
- 2 McMahon, D. G., Iuvone, P. M., Tosini, G. Circadian organization of the mammalian retina: from gene regulation to physiology and diseases. *Progress in Retinal and Eye Research*. **39** 58-76 (2014).
- 3 Prigge, C. L. et al. M1 ipRGCs Influence Visual Function through Retrograde Signaling in the Retina. *Journal of Neuroscience*. **36** (27), 7184-7197 (2016).
- 4 Zhang, D. Q., Belenky, M. A., Sollars, P. J., Pickard, G. E., McMahon, D. G. Melanopsin mediates retrograde visual signaling in the retina. *PLoS One*. **7** (8), e42647 (2012).
- 5 Liu, L. L., Alessio, E. J., Spix, N. J., Zhang, D. Q. Expression of GluA2-containing calcium-impermeable AMPA receptors on dopaminergic amacrine cells in the mouse retina. *Molecular Vision*. **25** 780-790 (2019).

- 6 Liu, L. L., Spix, N. J., Zhang, D. Q. NMDA Receptors Contribute to Retrograde Synaptic  
Transmission from Ganglion Cell Photoreceptors to Dopaminergic Amacrine Cells. *Frontiers in  
Cellular Neuroscience*. **11** 279 (2017).
- 7 Chung, K. et al. Structural and molecular interrogation of intact biological systems. *Nature*.  
**497** (7449), 332 (2013).
- 8 Poguzhelskaya, E., Artamonov, D., Bolshakova, A., Vlasova, O., Bezprozvanny, I. Simplified  
method to perform CLARITY imaging. *Molecular Neurodegeneration*. **9** 19 (2014).
- 9 Epp, J. R. et al. Optimization of CLARITY for Clearing Whole-Brain and Other Intact Organs.  
*eNeuro*. **2** (3) (2015).
- 10 Magliaro, C. et al. Clarifying CLARITY: Quantitative Optimization of the Diffusion Based  
Delipidation Protocol for Genetically Labeled Tissue. *Frontiers in Neuroscience*. **10** 179 (2016).
- 11 Yang, B. et al. Single-cell phenotyping within transparent intact tissue through whole-body  
clearing. *Cell*. **158** (4), 945-958 (2014).
- 12 Zheng, H., Rinaman, L. Simplified CLARITY for visualizing immunofluorescence labeling in the  
developing rat brain. *Brain Structure and Function*. **221** (4), 2375-2383 (2016).
- 13 Witkovsky, P., Arango-Gonzalez, B., Haycock, J. W., Kohler, K. Rat retinal dopaminergic  
neurons: differential maturation of somatodendritic and axonal compartments. *Journal of  
Comparative Neurology*. **481** (4), 352-362 (2005).

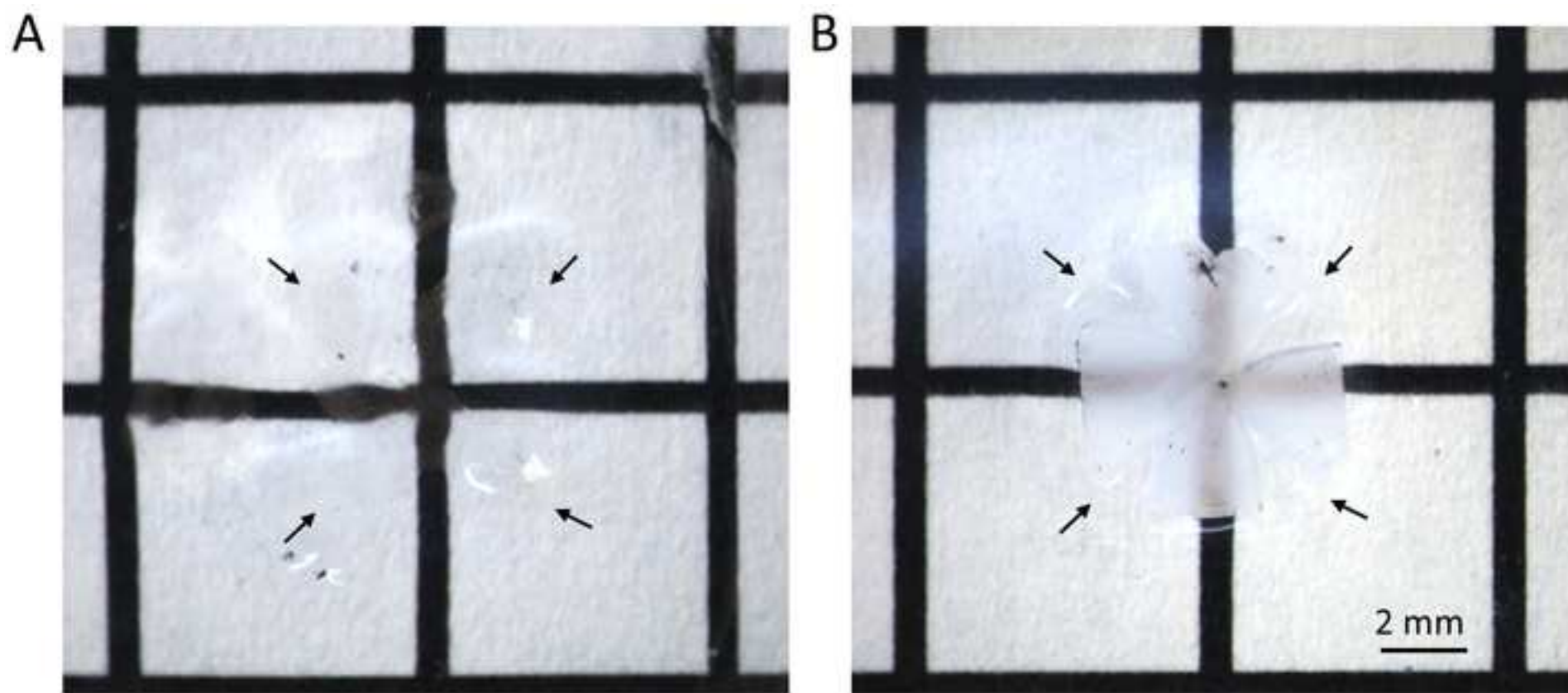


Figure 2

[Click here to access/download;Figure;Figure 2.jpg](#)

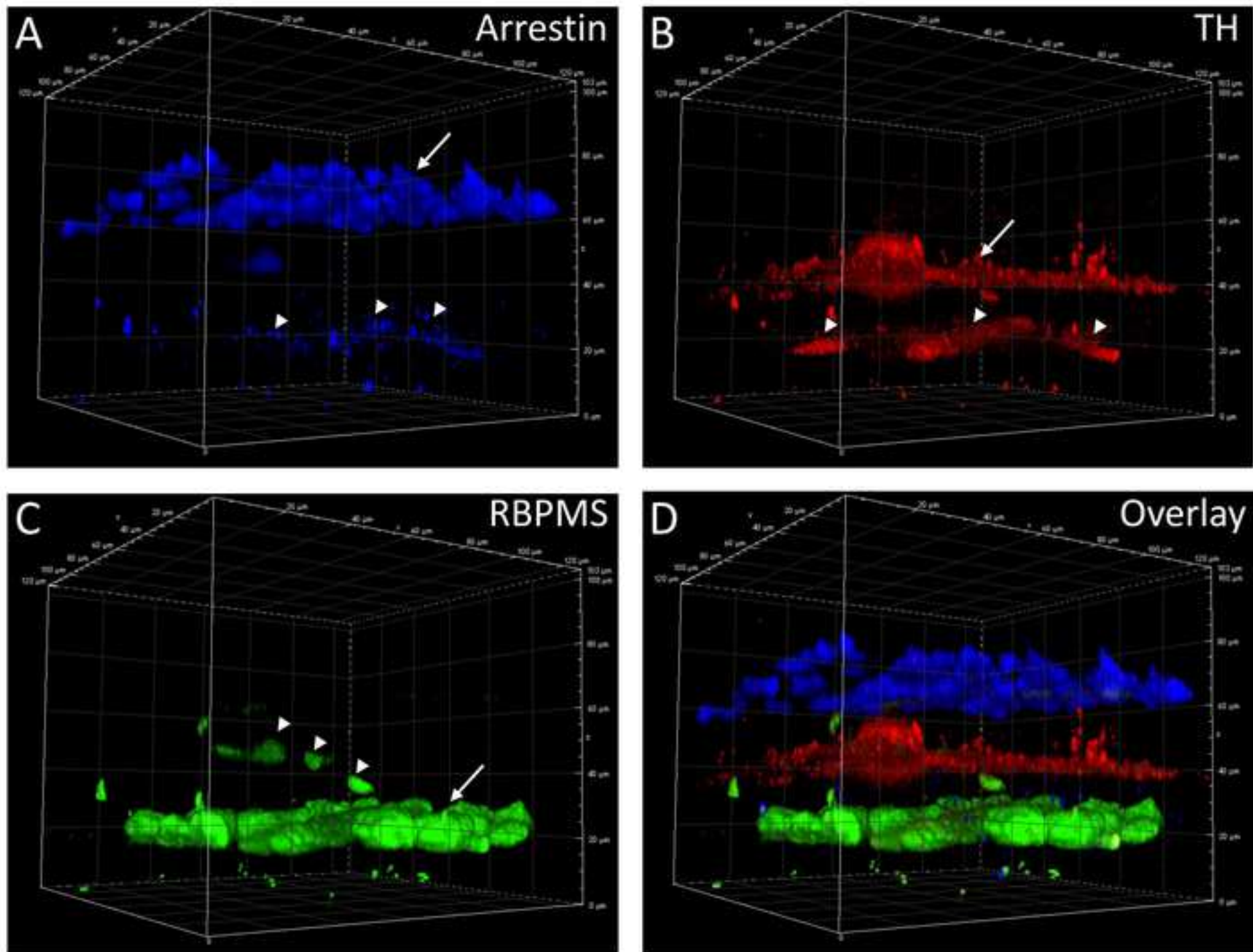




Figure 3

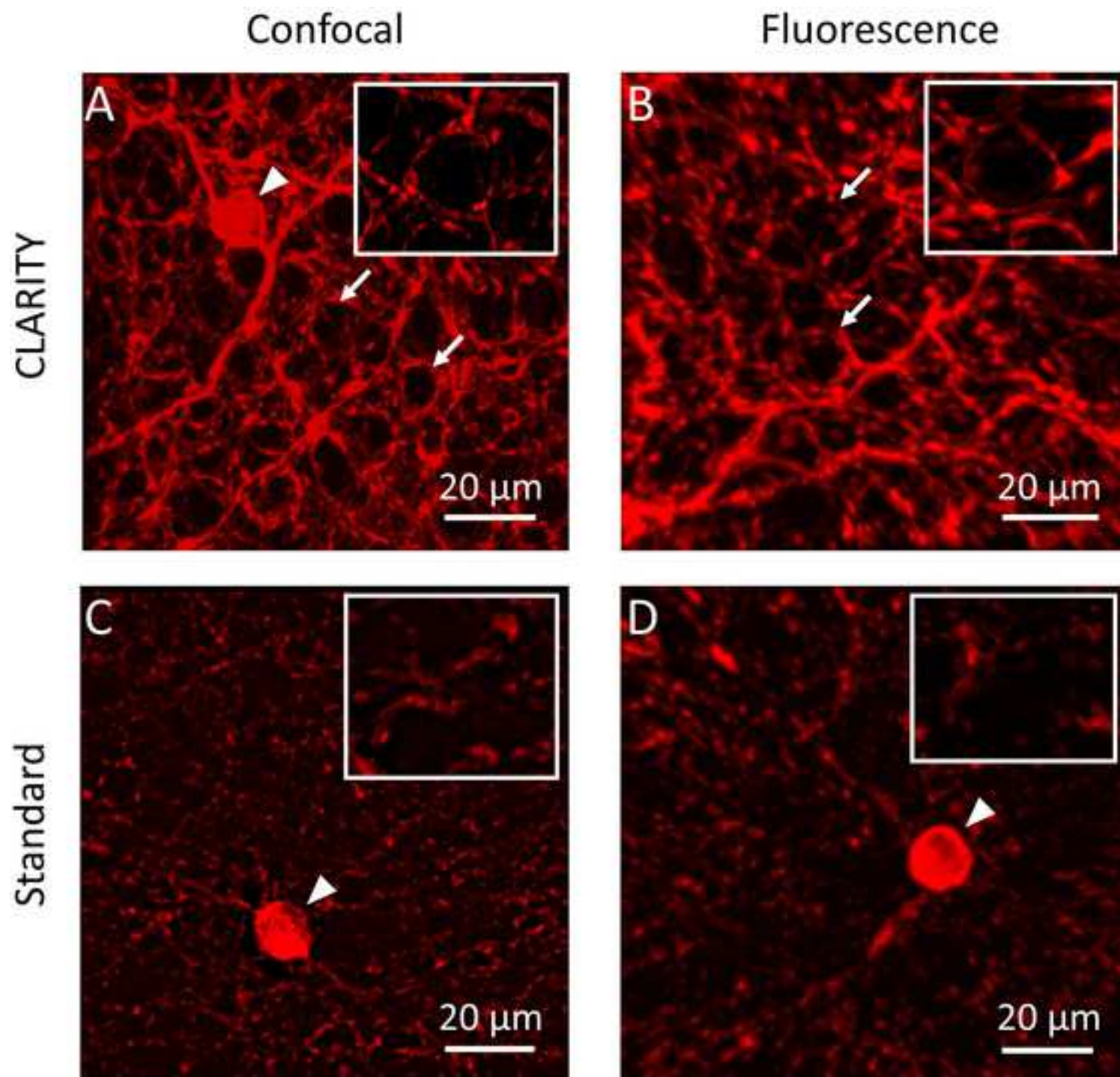


Figure 4

[Click here to access/download;Figure;Figure 4.jpg](#) 

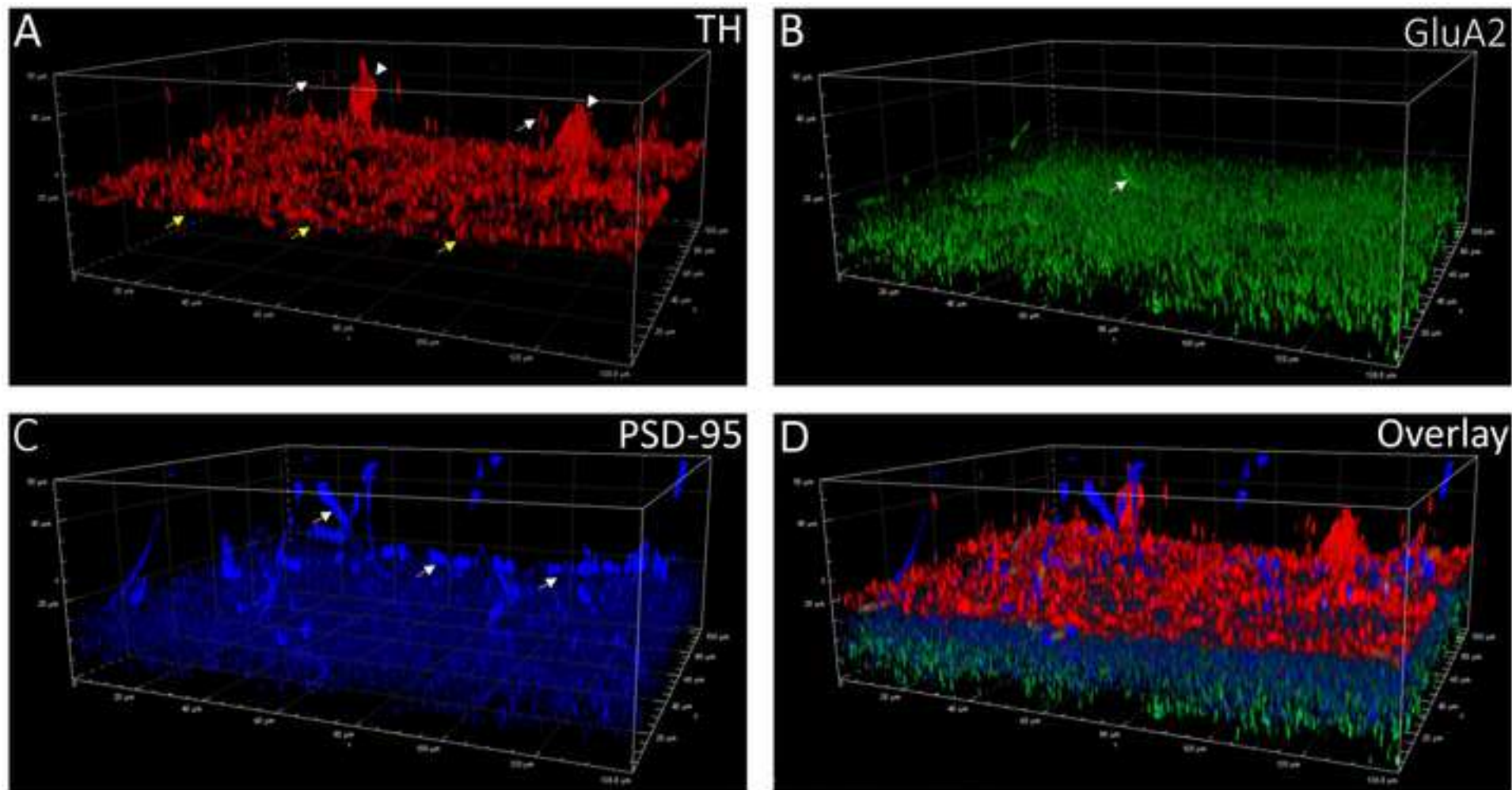
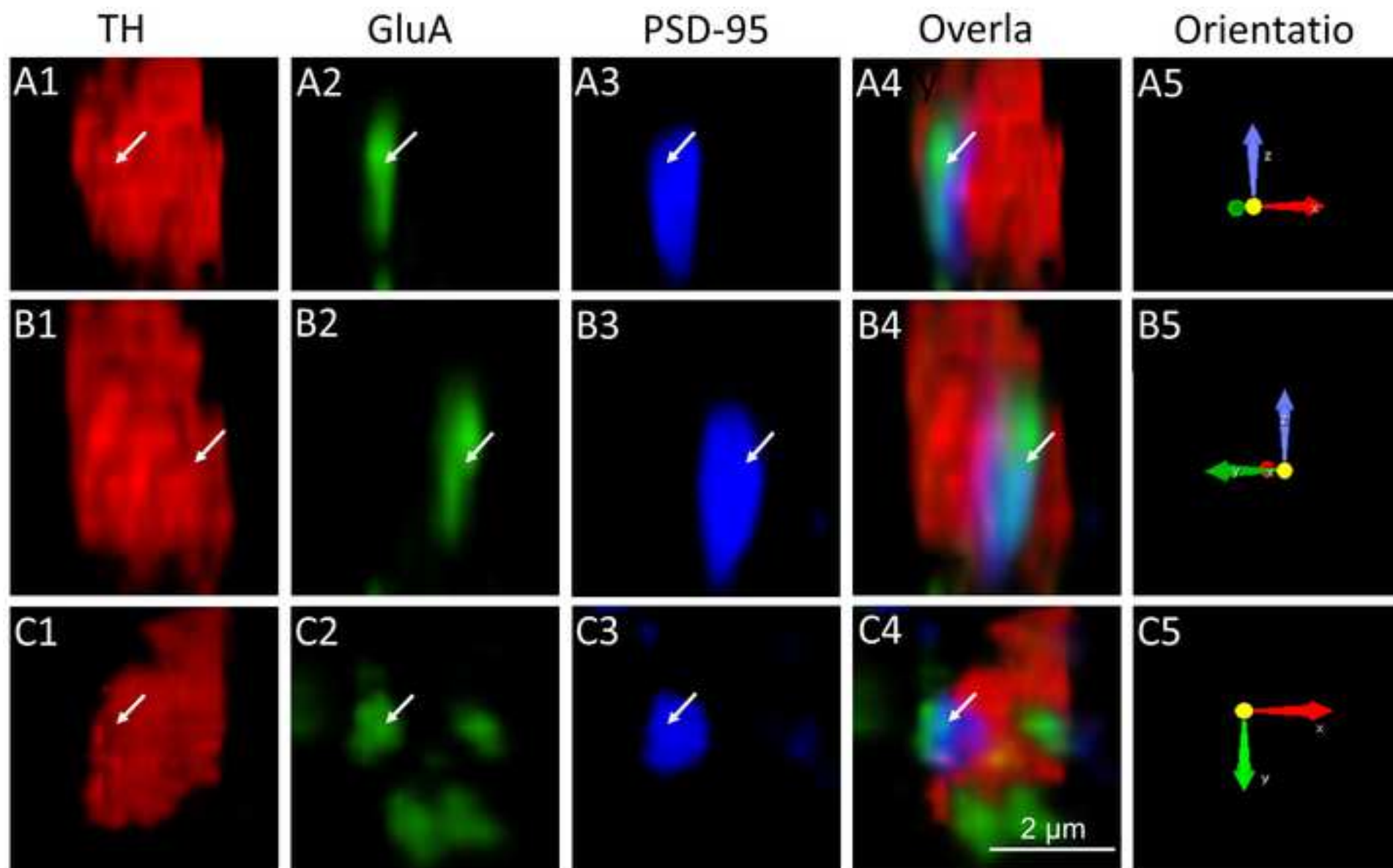


Figure 5

[Click here to access/download;Figure;Figure 5.jpg](#)





Solution	Compositic Notes
0.1 M PBS	137 mM NaCl Adjust pH to 7.4 26.8 mM KCl 10.1 mM Na <sub>2</sub> HPO <sub>4</sub> 17.6 mM KH <sub>2</sub> PO <sub>4</sub>
A4PO	4% acrylamide Prepare on ice, aliquot, and store at -20 °C 0.25% VA-044 0.1 M PBS
PBST	0.1% (v/v) Triton-X-100 0.1 M PBS
Blocking so	2% NDS or 1% BSA 0.01% NaN <sub>3</sub> PBST
0.1 M Phos	11.93 g NaCl Adjust pH to 7.5 15.34 g NaH <sub>2</sub> PO <sub>4</sub> /liter ddH <sub>2</sub> O
sRIMS	70% sorbitol Adjust pH to 7.5 with NaOH 0.1% tween-20 0.01% NaN <sub>3</sub> 0.02 M phosphate buffer

Antibody	IHC	Host	Dilution	Catalog #	Supplier	Ab registry	Target
Blue-sensit		+3 Goat polycl	1:1000	SC-14363	Santa Cruz	AB_215833	S-cone
Cone arrestin		+2 Rabbit polycl	1:1000	AB15282	EMD Millip	AB_116338	Cone
Protein kinase C		+3 Rabbit polycl	1:1000	SC-208	Santa Cruz	AB_216866	Rod bipolar cell
Glial fibrillary acidic protein		+3 Goat polycl	1:500	SC-6170	Santa Cruz	AB_641021	Astrocyte
Tyrosine hydroxylase		+3 Sheep polycl	1:500	AB1542	EMD Millip	AB_90755	Dopaminergic amacrine cell
Tyrosine hydroxylase		+2 Rabbit polycl	1:500	OPA1-0405	ThermoFisher	AB_325653	Dopaminergic amacrine cell
Choline acetyltransferase		+1 Goat polycl	1:500	AB144P	EMD Millip	AB_207975	Starburst amacrine cell
RNA-binding protein		+1 Guinea pig	1:2000	ABN1376	EMD Millip	AB_268740	Retinal ganglion cell
GluA2		+3 Rabbit polycl	1:500	AB1768-I	EMD Millip	AB_224787	Ca <sup>2+</sup> -impermeable AMPA receptor
GluA2		+2 Mouse monoclonal	1:250	MABN1189	EMD Millip	AB_273707	Ca <sup>2+</sup> -impermeable AMPA receptor
Postsynaptic density		+3 Mouse monoclonal	1:1000	75-028	NeuroMab	AB_287718	Synaptic sites
Phosphoserine		0 Rabbit polycl	1:500	44-923G	ThermoFisher	AB_253379	Cell activity marker

e cell

e cell

I

IPA receptor

IPA receptor

Table 3

Host	Target species	Conjugate	Dilution	Supplier
Donkey	Anti-sheep	Alexa Fluor 1:500		Invitrogen
Donkey	Anti-sheep	Alexa Fluor 1:500		Invitrogen
Donkey	Anti-rabbit	Alexa Fluor 1:500		Invitrogen
Donkey	Anti-rabbit	Alexa Fluor 1:500		Invitrogen
Goat	Anti-rabbit	Alexa Fluor 1:500		Invitrogen
Donkey	Anti-mouse	Alexa Fluor 1:500		Invitrogen
Donkey	Anti-mouse	Alexa Fluor 1:500		Invitrogen
Donkey	Anti-goat	Alexa Fluor 1:500		Invitrogen
Donkey	Anti-goat	Alexa Fluor 1:500		Invitrogen
Goat	Anti-guinea pig	Alexa Fluor 1:500		Invitrogen

Name of Material/Equipment	Company	Catalog Number	Comments/Description
16% Paraformaldehyde	Electron Microscopy Sciences	15710	Fixative
Acrylamide	Fisher Biotech	BP170	Hydrogel monomer
Axio Imager.Z2	Zeiss		Fluorescence microscope
BSA	Fisher Scientific	BP1600	Blocking agent
Eclipse Ti	Nikon Instruments		Scanning confocal microscope
KCl	VWR	BDH0258	Buffer component
KH <sub>2</sub> PO <sub>4</sub>	Sigma	P5655	Buffer component
Na <sub>2</sub> HPO <sub>4</sub>	Sigma Aldrich	S9763	Buffer component
NaCl	Sigma Aldrich	S7653	Buffer component
NaH <sub>2</sub> PO <sub>4</sub>	Sigma Aldrich	S0751	Buffer component
NaN <sub>3</sub>	Sigma Aldrich	S2002	Bacteriostatic preservative
NDS	Aurion	900.122	Blocking agent
NIS Elements AR	Nikon		Image analysis software
SDS	BioRad	1610301	Delipidation agent
Sorbitol	Sigma Aldrich	51876	Buffer component
Triton-X-100	Sigma	T8787	Surfactant
Tween-20	Fisher Scientific	BP337	Surfactant
VA-044	Wako Chemicals	011-19365	Thermal initiator

## Response to comments from Reviewers and the Editor

### Response to editorial comments:

1. Please take this opportunity to thoroughly proofread the manuscript to ensure that there are no spelling or grammar issues. Please define all abbreviations at first use.

**Response:** We have tried our best to limit spelling or grammar issues.

2. Please provide an email address for each author.

**Response:** Email addresses for both authors are provided on the face page of the manuscript.

3. Please rephrase the Summary to clearly describe the protocol and its applications in complete sentences between 10-50 words: "Here, we present a protocol to ..."

**Response:** As suggested, we have added a summary statement on lines 26-28. The abstract has also been revised (lines 36-45).

4. Please revise the text, especially in the protocol, to avoid the use of any personal pronouns (e.g., "we", "you", "our" etc.).

**Response:** We have changed them wherever needed.

5. Please ensure that all text in the protocol section is written in the imperative tense as if telling someone how to do the technique (e.g., "Do this," "Ensure that," etc.). The actions should be described in the imperative tense in complete sentences wherever possible. Avoid usage of phrases such as "could be," "should be," and "would be" throughout the Protocol. Any text that cannot be written in the imperative tense may be added as a "Note." However, notes should be concise and used sparingly. Please include all safety procedures and use of hoods, etc.

**Response:** We have revised wherever needed.

6. Please note that your protocol will be used to generate the script for the video and must contain everything that you would like shown in the video. Please add more details to your protocol steps. Please ensure you answer the "how" question, i.e., how is the step performed? Alternatively, add references to published material specifying how to perform the protocol action. Please add more specific details (e.g., button clicks for software actions, numerical values for settings, etc) to your protocol steps. There should be enough detail in each step to supplement the actions seen in the video so that viewers can easily replicate the protocol.

**Response:** We have considered the suggestion while revising the manuscript.

7. Line 96: Please specify the method of euthanasia without highlighting it.

**Response:** We have added the method of euthanasia (line 111).

8. Please provide solution composition (Solutions sub-section of the protocol) as a Table in a separate .xls or .xlsx file uploaded to your Editorial Manager account. This table can then be referenced in the protocol text. Reagents and equipment needed can be listed assay-wise in the Table of Materials. For example, line 167, you can simply enter NIS Elements AR in the Table of Materials and add the comment that it was used for image analysis and remove the mention from the protocol while citing Table of Materials.

**Response:** We have added a new table (Table 1) with solution composition and referred the Table wherever needed throughout the manuscript. Table of Materials has also been revised and cited wherever needed.

9. Line 122: what is the composition of your blocking solution?

**Response:** The composition of the blocking solution has been added to a new Table 1.

10. Please format the manuscript as: paragraph Indentation: 0 for both left and right and special: none, Line spacings: single. Please include a single line space between each step, substep and note in the protocol section. Please use Calibri 12 points and one-inch margins on all the side. Please include a one line space between each protocol step and then highlight up to 3 pages of protocol text for inclusion in the protocol section of the video.

**Response:** We have reformatted the manuscript as suggested.

11. As we are a methods journal, please revise the Discussion to explicitly cover the following in detail in 3-6 paragraphs with citations:

- a) Critical steps within the protocol
- b) Any modifications and troubleshooting of the technique
- c) Any limitations of the technique
- d) The significance with respect to existing methods
- e) Any future applications of the technique

**Response:** We have revised the Discussion as suggested. We have added a new paragraph describing the consideration, limitation, and future application of the protocol (lines 404-425).

12. Please move figure and table legends to a section “figure and table legends” between representative results and discussion sections.

**Response:** Done.

13. Please do not abbreviate journal names in the reference list.

**Response:** Citations have been edited to include full journal names.

14. Please sort the Materials Table alphabetically by the name of the material.

**Response:** Done.

#### **Response to Reviewer #1's comments**

1. A Figure with imaging performed on the control (i.e. non clarified tissues) should be provided.

**Response:** Thank you for the suggestion. We have revised Figure 3 by adding immunostaining for dopaminergic amacrine cells taken from non-clarified whole-mount retinas (Figures 3C and D). In the same figure, we have added new figures to compare an image taken from confocal with that from fluorescence microscopy. The description (lines 258-268) and figure legend for Figure 3 have also been revised.

2. Information about tissue expansion due to the clarification procedures should be provided.

**Response:** This is an excellent suggestion. We have discussed this issue in Discussion (lines 410-414).

#### **Response to Reviewer #2's comments**

1. The method of mounting the retina onto the slide (Mounting step #6, line 146) is a bit confusing. "Place a stack of 3 coverslips on each side of the mounted retina. Use the long edge of another slide to press down the coverslip so that the mount is flat and even". Unclear what is the point of placing the stack of 3 coverslips on the back of the slide. I assume these additional 6 coverslips are removed after flattening the retina. A diagram would be really useful to illustrate this - I understand that a video will be produced, but a diagram in the printed manuscript would be quite useful.

**Response:** We used a stack of 3 coverslips as a spacer. We have clarified this in the protocol (line 183) and will demonstrate the procedure in the video.

2. Fig2 includes an arrow head pointing out "non-specific, cross reactivity, spectral bleeding". There should not be a spectral bleeding problem in confocal images if the potentially photo bleeding channels are imaged sequentially. Cross reactivity should not have occurred, if the primary and secondary antibodies are specific.

**Response:** Non-specific blood vessel staining was observed in our images because we did not perfuse the whole animal with intracardiac perfusion method before getting the eyes out. We



have discussed this issue and suggested that intracardiac perfusion of the animals may need to avoid non-specific staining in CLARITY-processed retinas in the revision (lines 419-421).

3. While the cleared retina tissue is refractive index matched, the imaging medium and its interface with the microscope camera is likely not (air or oil lens? not mentioned), because the glass coverslip will refract light. However, these problems may be minor as the retinas are only 300um thick. CLARITY is often used for quite thicker samples, and in those cases a microscope objective with "dipping lens" placed directly into the medium is best (i.e., no coverslip). The authors should consider explaining why a coverslip was used here, and what its limitations may be when imaging other (thicker) samples.

**Response:** This is a good question. We have discussed this issue in the Discussion section (lines 414-418).

4. This report is not the first to use passive clearing of fragile tissues for CLARITY, and is not the first to use an oil overlay rather than nitrogen de-gassing during hydrogel polymerization. Citations to previous reports should be included (e.g., <https://pubmed.ncbi.nlm.nih.gov/25772507/> and [http://wiki.claritytechniques.org/index.php/Hydrogel\\_Embedding](http://wiki.claritytechniques.org/index.php/Hydrogel_Embedding) )

**Response:** Thank you for the suggestion. We have included citations for the passive clearing.

5. Some of the reagents included in the Table were cut-off, perhaps due to formatting problem when converting to PDF. Ab registry numbers should be included for all primary antibodies (<https://antibodyregistry.org/> )

**Response:** We have included Antibody Registry numbers in new Table 2.

### **Response to Reviewer #3's comments**

1. Whether the CLARITY process distorts the tissue is a concern. Figure 4 may rule out the concern, which exhibits homogeneous and flat distributions of TH and GluA2. In some ways, please address if the CLARITY process does or does not distort the tissue.

**Response:** Please see the response to comment #1 of Reviewer #1.

2. The penetration of antibodies is also an issue for immunostaining with wholemount tissue. Please present the penetration improvement by CLARITY. For example, PSD-95 penetration to deep into the tissue may not occur in the normal retinal tissue. Alternatively, the amount of antibody can be reduced.

**Response:** Upon immunostaining for PSD-95 and GluR2 with standard whole-mount tissue, we observed little to no labeling of these subcellular structures in the deep layers of the retina, suggesting poor antibody penetration. As demonstrated in the manuscript, this application of

the CLARITY protocol allows distinct staining of these proteins in the inner retinal layers, indicating improved antibody penetration to the deep tissue. We have discussed this issue on lines 391-394.